Asian Journal of Chemistry; Vol. 38, No. 4 (2026), 938-948
ASIAN JOURNAL OF CHEMISTRY
https://doi.org/10.14233/ajchem.2026.35460

Green Synthesis and Characterisation of Silver Nanoparticles using Tuber Extract of *Drynaria quercifolia* (L.) J.Sm.: *In vitro* Cytotoxicity Activity against Human Liver Cancer (HepG2) Cells

ASI THOMAS[1], KALAISELVAN SELVARAJ[1], RAJENDRAN VENKATESH[2,*], M. MANGALAM[3,*], ASHMITHA ELANGOVAN[4] and NIRUBAMA KUMAR[1]

[1]Department of Biochemistry, Kongunadu Arts and Science College, Coimbatore-641029, India
[2]Department of Saveetha College of Nursing, Saveetha Institute of Medical and Technical Sciences, Chennai-602106, India
[3]Department of Chemistry, Rajah Serfoji Government College, Thanjavur-613005, India
[4]Department of Zoology, PSGR Krishnammal College of Women, Coimbatore-641004, India

*Corresponding authors: E-mail: venkatbiochem11@gmail.com; mangalampasu18@gmail.com

Received: 15 December 2025 *Accepted*: 4 February 2026 *Published online*: 8 April 2026 AJC-22314

Nanomedicine enables targeted drug delivery within the tumor microenvironment and shows considerable promise for the treatment of hepatocellular carcinoma (HCC). This study investigates the phytoconstituents of *Drynaria quercifolia*, which are known for their antioxidant, antimicrobial, and anti-inflammatory activities. In addition, silver nanoparticles (Ag NPs) were synthesized from the tuber extract of *D. quercifolia* and their apoptotic and cytotoxic effects were evaluated. The results demonstrated that the high concentrations of phenols and flavonoids contribute significantly to antioxidant activity, with IC_{50} values of 223.70 µg/mL in the DPPH assay and 208.56 µg/mL in the $ABTS^+$ assay, values that are comparable to the standard IC_{50}. The formation of silver nanoparticles was confirmed by UV-visible spectroscopy, which showed a characteristic absorption peak at 445 nm. FTIR spectroscopy indicated the presence of O–H functional groups, while SEM analysis revealed crystalline nanoparticles with an approximate size of 40 nm. Furthermore, cytotoxicity assays clearly demonstrated a dose-dependent decrease in the viability of HepG2 cells. Similar observations were obtained in apoptosis assays using Ag NPs.

Keywords: *Drynaria quercifolia*, Silver nanoparticles, Liver cancer, Cytotoxicity.

INTRODUCTION

Metal nanoparticles (MNPs) have attracted a lot of interest due to their unique physico-chemical characteristics, small size and reliable behaviour [1,2]. These special qualities provide metal nanoparticles with interesting new opportunities in water treatment, antimicrobial applications, optical devices, targeted medication delivery, cancer therapy and catalysis [3,4]. Silver nanoparticles (Ag NPs) are unique among other metal nanoparticles including Pd, Cu, Au, Zn, Sn, Ag and Co, due to their wide range of applications in many industries [5].

In the context of green synthesis, metal ions are naturally reduced by biomolecules in plants and microbes, which results in the production of metal nanoparticles [6]. Several research groups have recently produced Ag NPs using the green synthesis approach and their photophysical and morphological properties have been established [7-10]. Due to its environmental friendliness, sustainability, energy efficiency and economic viability, the use of medicinal plant extracts as the main source in the green synthesis method for Ag NPs has attracted significant interest in a variety of medical applications [11]. The intrinsic complexity and diversity of phytochemical ingredients provide serious complications to the standardisation and repeatability of green synthesis techniques, notwithstanding the promise biomedical applications [12].

Cancer is one of the most causes of death in the world wide approximately one in six fatalities or 9.6 million people in 2018 alone. However, 70% of cancer-related deaths take place in middle- and low-income countries. The most prevalent form of liver cancer, hepatocellular carcinoma (HCC), ranks sixth in terms of prevalence and is the fourth major cause of cancer-related deaths globally [13]. Nanotechnology-based therapeutic and diagnostic methods have also demonstrated promise in recent years to enhance cancer treatment [14]. With an emphasis on the significant advancements in cancer detection, diagnosis and therapy, cancer nanotechnology

opened up a new avenue for interdisciplinary research in chemistry, medicine, engineering and biology [15-17] due to their unparalleled features, high reactivity and enormous surface area to volume ratio [18,19]. Recently, methods for synthesizing Ag NPs using green chemistry have showed a lot of promise in addressing this problem [20]. Ag NPs can induce cytotoxicity in cancer cells by changing their shape, decreasing their viability and causing oxidative stress in certain cancer cells. Moreover, Ag NPs cytotoxic actions also play a critical role in tumor management [21,22].

Drynaria quercifolia widely used in the traditional medicine for the treatment of cough, fever, dyspepsia, diarrhea, tuberculosis, typhoid, cholera, jaundice, fever, headaches, skin conditions and syphilis. Additionally, it has been found that the plant helps repair and strengthen bones, muscles and sinews [22,23]. The extensive phytochemical profile of *D. quercifolia*, which includes flavonoids, alkaloids, terpenoids, tannins, saponins, quinones, glycosides and polyphenols, accounts for its medicinal importance. Moreover, the methanolic extract of leaves of *D. quercifolia* showed potent cytotoxic activity and *D. quercifolia* rhizome extract phytocompounds showed potential antiproliferative activity against A549 lung cancer cells [24]. In the current investigation, we aimed to study the anticancer potential of green-synthesised Ag NPs from *D. quercifolia* tuber on HepG2 cells (human hepatocellular adenocarcinoma cell line).

EXPERIMENTAL

Collection and identification of rhizome: The tubers of *Drynaria quercifolia* were collected from Eastern ghats in Tamil Nadu state, India and authenticated by the qualified botanist. The obtained rhizomes were washed thoroughly with tap water to remove soil. The tubers were cut into small pieces and shade dried. Then the dried tubers were ground into coarse powder and collected in an air-tight container.

Solvent extraction: The powdered *D. quercifolia* were packed in Soxhlet apparatus for the successive extraction procedure with the following solvents such as ethanol, chloroform, acetone, hexane and aqueous. For aqueous extract, the rhizome powder decoction was made with boiling water and constantly stirred for 30 min and filtered. The solvent extraction was prepared under low pressure in a vacuum evaporator and air dried. Stock solutions of each extract were prepared as 1 mg/mL and stored for further analysis.

Qualitative phytochemical analysis: The qualitative phytochemical analyses of aqueous, ethanol, chloroform, acetone and hexane extracts were performed using standard protocols reported by Peach & Tracey [25] and Raaman [26] to determine the presence of major bioactive compounds, including alkaloids, flavonoids, tannins, saponins, steroids, terpenoids, glycosides, phenols, carbohydrates and proteins.

Antioxidant activity: The antioxidant property of *D. quercifolia* extracts were evaluated to assess the free radical scavenging capacity that mitigate the oxidative stress by various assays such as DPPH, ABTS, superoxide radical scavenging activity, nitric oxide scavenging and reducing power assay.

DPPH radical scavenging assay: The antioxidant activity by unstable radical scavenging assay using stable DPPH and the absorbance was read at 517 nm against the control BHT. The antioxidant activity is based on the DPPH inhibition by ethanolic extract [26].

$ABTS^+$ radical scavenging activity: The scavenging activity was determined by ABTS radical cation scavenging action by ethanolic extracts. $ABTS^+$ solution was prepared into different concentration from 5-100 μg/mL. The ethanolic mixture of sample extracts were added to the tubes and incubated for 6 min against the standard ascorbic acid. The absorbance was read at 734 nm [27].

Superoxide radical scavenging activity: This method is based on the inhibition of production of nitro blue tetrazolium of the superoxide ion by the plant extract and was measured spectrophotometrically at 560 nm. The initial optical uniformly with a fluorescent lamp for 30 min. A 560 nm was measured again and difference in optical density was taken as the quantum of superoxide production. The percentage inhibition was calculated by comparing with the optical density of the control tubes [28].

$$\text{Radical scavenging activity (\%)} = \frac{\text{Control} - \text{Sample}}{\text{Control}} \times 100$$

Nitric oxide (NO) scavenging activity: The interaction of sample with nitric oxide was assessed by the nitride detection method. Nitric oxide was generated from sodium nitroprusside and measured by Griess illosvoy reaction. Nitric oxide generated from sodium nitroprusside in aqueous solution at physiological pH interacts with oxygen to produce nitrite ions which were measured at 540 nm against blank. 0.5 mL of the reaction mixture containing nitrite was removed, 1.0 mL of sulphanilic acid reagent was added, mixed well and allowed to stand for 5 min for completion of diazotisation and 1.0 mL of naphthyl ethylenediamine dihydrochloride was added, mixed well and allowed to stand for 30 min in diffused light. A pink colour chromophore was formed [29]. Rutin was used as a standard. The inhibition was calculated according to the equation:

$$\text{I (\%)} = \frac{A_o - A_1}{A_o} \times 100$$

where A_o is the absorbance of control reaction and A_1 is the absorbance of test compound.

Reducing power assay: The ethanolic extracts at different concentrations of 2.5 mL added with 2.5 mL of 1% potassium ferricyanide and 2.5 mL of 0.2 M sodium phosphate buffer made up the reaction mixture. Except sample all the reagent must be present in the control. After 20 min of incubation at 50 ºC, 2.5 mL of 10% (w/v) trichloroacetic acid was added and the mixture was centrifuged for 10 min at 3000 rpm. Then, 1 mL of 0.1% $FeCl_3$, 5 mL of deionised water and 5 mL of supernatant upper layer were mixed. The absorbance was measured at 700 nm against blanks with phosphate buffer and distilled water.

Synthesis of Ag NPs: Silver nitrate solution (1 mM) 100 mL was slowly mixed with 10 mL of *D. quercifolia* ethanolic extract and then placed in dark room at the room temperature for 24 h. The formation Ag NPs were confirmed by the change in the colour from brown colour to dark brownish colour.

Characterisation: UV–Visible spectroscopy was used to confirm nanoparticle formation by recording the absorbance spectrum of the colloidal sample in the range of 200-800 nm using a Shimadzu UV-1800 spectrophotometer with distilled water as reference. FTIR analysis (FTIR RX1, Perkin-Elmer) was performed in the 4000-400 cm^{-1} region to identify the functional groups in *D. quercifolia* responsible for metal ion reduction and nanoparticle stabilization and emission spectra were recorded using a Perkin-Elmer LF-45 fluorescence spectrophotometer. X-ray diffraction (XRD) of the powdered nanomaterial was analyzed using a Bruker AXS diffractometer over a 2θ range of 10-80º. The morphology of the synthesized Ag NPs was examined using scanning electron microscopy (SEM) at 120 kV (JEOL, Tokyo, Japan) and elemental composition was determined by energy-dispersive X-ray spectroscopy (EDAX) using a SUPRA 55 SEM equipped with an EDAX detector.

Cell culture: HepG2 cells were obtained from the National Centre for Cell Sciences in Pune, India and cultured in DMEM media supplemented with 10% fetal bovine serum (FBS), 100 U/mL of streptomycin and penicillin and 5% CO_2 at 37 ºC.

Cytotoxic activity: The MTT assay was used to assess the cytotoxic effect of Ag NPs against HepG2 cells [30]. Ag NPs treated cells (5×10^6 cells/well) and control cells were plated in 96-well plates with 200 µL of media in each well. After incubation, the medium was removed, 200 µL of MTT solution (5 mg/mL) was added and wells were washed twice or three times using PBS. The plates were kept in an incubator with 5% CO_2 for 5 h. After dissolving the crystals in 1 µL of DMSO, the colour turned purple, signifying the presence of living cells. The absorbance of the cell suspension was measured at 595 nm, with DMSO acting as a blank. Plotting drug concentration and cell viability on the *x*-axis and *y*-axis, respectively, allowed for the graphic calculation of the IC_{50} value.

Ethylene bromide and acridine orange staining: After treating HepG2 cells (5×10^6 cells/well) with Ag NPs for 24 h and incubating the control (25 µL), 1 µL of acridine orange/ethidium bromide (AO/EB) solution was added prior to the microscopic examination. In the fluorescence microscope, the samples under the cover slip were analysed to look for at least 100 cells.

Measurement of mitochondrial membrane potential: The mitochondrial membrane potential of HepG2 cells treated with Ag NPs was assessed by MMP assay kit (Sigma, USA). After a 24 h incubation period, the Ag NPs treated HepG2 cells and control cells were taken out and incubated for 60 min in the dark at 37 ºC in a humidified 5% CO_2 environment with 100 µL of JC-10 dye loading solution. Each sample received 100 µL of buffer after incubation. After centrifuging the plate for 2 min at 800 rpm, the fluorescence was measured at the ratios of 490/525 and 540/590.

RESULTS AND DISCUSSION

Plant secondary metabolites are an important source of bioactive compounds and have gained considerable attention due to their potential role in the development of plant-derived therapeutic agents. Phytochemical screening (Table-1) in this study revealed the presence of alkaloids, phenols, saponins, flavonoids, tannins, terpenoids, proteins and carbohydrates in ethanol, chloroform, acetone, hexane and aqueous extracts. Alkaloids, flavonoids, carbohydrates, phenols and steroids were detected in all extracts, while the aqueous extract showed comparatively lower levels of flavonoids, phenols and alkaloids. Whereas glycosides and amino acids were present in higher concentrations in methanol, hexane, acetone and aqueous extracts but were lower in chloroform extract. Consistent with previous reports, ethanol extracts showed relatively higher concentrations of saponins, terpenoids, flavonoids and tannins.

DPPH radical scavenging assay: The DPPH radical scavenging activity of the ethanolic extract of *D. quercifolia* was evaluated at different concentrations (50, 100, 150, 200, and 250 µg/mL), with butylated hydroxytoluene (BHT) used as the standard. As shown in Fig. 1, the percentage inhibition of DPPH radicals increased progressively with increasing concentrations of the extract, indicating a concentration-dependent antioxidant activity. The free radical scavenging ability was determined by the reduction of the stable DPPH radical to yellow-coloured 1,1-diphenyl-2-picrylhydrazine, and the absorbance was measured at 515 nm using a spectrophotometer. The IC_{50} value of the ethanolic extract was found to be 223.70 µg/mL, whereas the standard BHT exhibited an IC_{50} value of 161.65 µg/mL. The observed antioxidant activity

TABLE-1
IDENTIFICATION OF PHYTOCONSTITUENTS PRESENT IN DIFFERENT SOLVENT EXTRACTS OF *Drynaria quercifolia* TUBERS

Phytochemicals	Ethanol	Chloroform	Acetone	Hexane	Water
Alkaloids	+++	++	+++	+	++
Phenols	+++	+++	+++	++	+
Flavonoids	+++	+++	+++	++	+
Tannins	++	–	+	+	+
Saponins	+	–	+	+	–
Terpenoids	++	–	+	++	++
Steroids	++	++	++	+++	++
Carbohydrates	++	+	++	+++	++
Glycosides	++	+	++	+++	++
Amino acids	++	+	+++	+++	++
Proteins	++	+	++	+++	++

(+) small concentration; (++) moderately high concentration; (+++) very high concentration; (–) absent

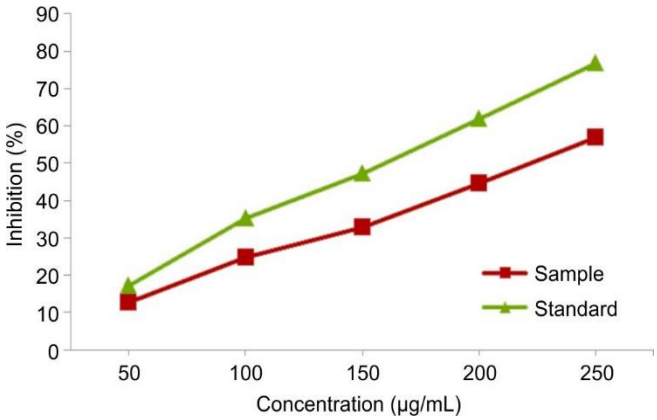

Fig. 1. DPPH scavenging assay of ethanolic extract of *D. quercifolia*

of the extract may be attributed to the high levels of phenolic and flavonoid compounds present in *D. quercifolia* [31].

ABTS$^+$ radical scavenging activity: The ABTS radical scavenging activity of the ethanolic extract of *D. quercifolia* was evaluated at different concentrations (50, 100, 150, 200, and 250 µg/mL), with vitamin C used as the standard. As shown in Fig. 2, the percentage inhibition increased with increasing concentrations of the extract, although the activity remained slightly lower than that of the standard at all concentrations. The results indicate that the extract possesses notable electron-donating ability, which can neutralize reactive oxygen and nitrogen species and may help reduce the formation of pro-inflammatory oxidants such as peroxynitrite ($ONOO^-$) [31]. The IC_{50} value of the ethanolic extract of *D. quercifolia* was 208.56 µg/mL, while the IC_{50} value of standard vitamin C was 185.39 µg/mL. The maximum radical scavenging activity was observed at 250 µg/mL, exhibiting 62.30 ± 0.40% inhibition.

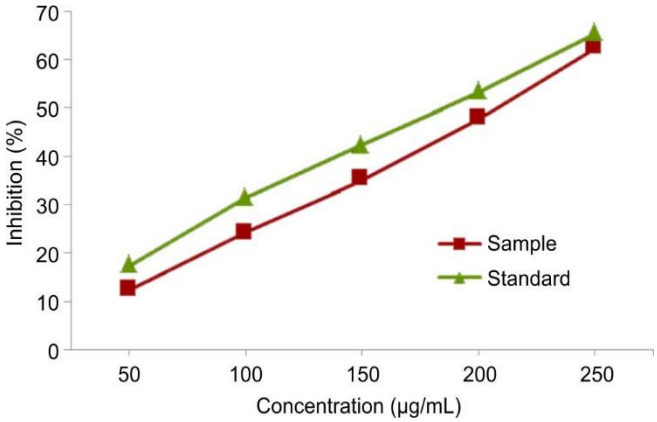

Fig. 2. ABTS$^+$ radical scavenging assay of ethanolic extract of *D. quercifolia*

Superoxide radical scavenging assay: The superoxide radical scavenging activity of the ethanolic extract of *D. quercifolia* was evaluated at different concentrations (50-250 µg/mL), using vitamin C as the standard. As shown in Fig. 3, the scavenging activity increased with increasing extract concentration, with the highest inhibition observed at 250 µg/mL (67.35 ± 0.45%). The antioxidant activity of the extract may be associated with the presence of phytocompounds such as flavonoids, including kaempferol, which are known to scavenge

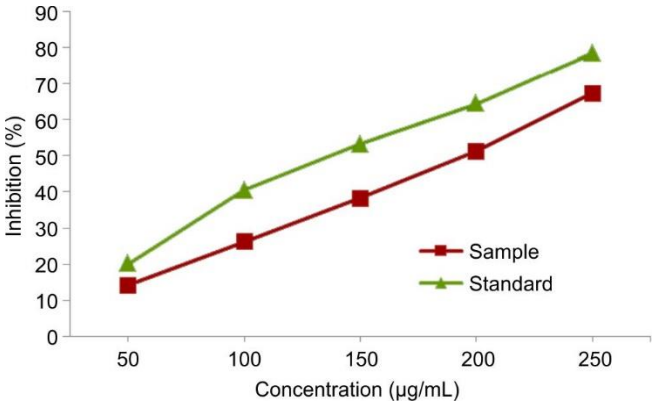

Fig. 3. Superoxide radical scavenging assay of ethanolic extract of *D. quercifolia*

superoxide radicals. Hydrogen peroxide is also considered harmful to cells even at low physiological concentrations (10-100 nM), since it can easily diffuse through the biological membranes and generate cytotoxic hydroxyl radicals [32]. The IC_{50} value of the ethanolic extract of *D. quercifolia* was 195.46 µg/mL, which was comparable to that of standard vitamin C (195.46 µg/mL), indicating significant antioxidant potential.

Nitric oxide scavenging assay: The nitric oxide scavenging activity of the ethanolic extract of *D. quercifolia* was evaluated at different concentrations (50-250 µg/mL), with rutin used as the standard. In this assay, antioxidants present in the extract compete with oxygen to react with nitric oxide, leading to a reduction in absorbance measured at 550 nm. As shown in Fig. 4, the percentage inhibition increased with increasing concentrations of the extract, although the activity remained slightly lower than that of the standard. The IC_{50} value of the ethanolic extract of *D. quercifolia* was 212.98 µg/mL, whereas the standard rutin exhibited an IC_{50} value of 189.19 µg/mL. Since nitric oxide can exert various cytotoxic effects under physiological conditions, plant extracts demonstrating significant nitric oxide scavenging activity may serve as potential sources of natural antioxidant compounds [33].

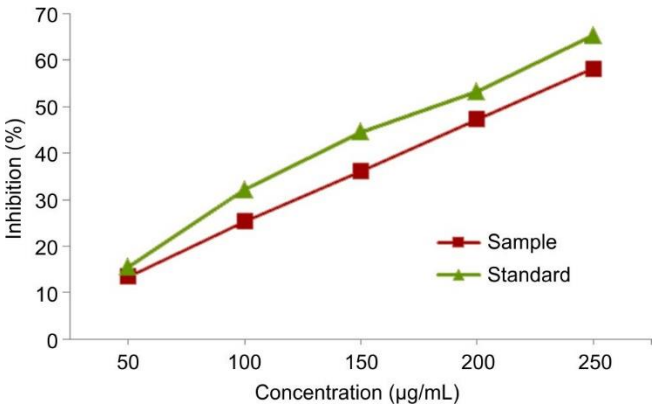

Fig. 4. Nitric oxide scavenging assay of ethanolic extract of *D. quercifolia*

Reducing power assay: The ferric reducing power of the ethanolic extract of *D. quercifolia* was evaluated at the different concentrations (50-250 µg/mL) and compared with the standard vitamin C. All experiments were performed in triplicate. As shown in Fig. 5, the reducing power increased with

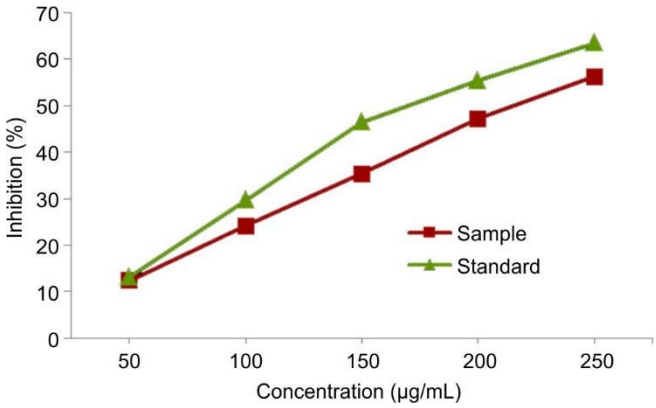

Fig. 5. Reducing power assay of ethanolic extract of *D. quercifolia*

increasing concentrations of the extract, indicating a concentration-dependent antioxidant activity, although the activity remained slightly lower than that of the standard. The IC_{50} value of the ethanolic extract was 213.93 µg/mL, while the IC_{50} value of vitamin C was 166.03 µg/mL. The enhanced reducing capacity may be attributed to the presence of phytochemical constituents such as phenolic and flavonoid compounds, which are known to contribute significantly to antioxidant activity [34].

GC-MS: Several bioactive molecules were found in GC-MS analysis and the results are depicted in Table-2. The ethanolic extract of *D. quercifolia* exhibit about 32 different compounds (Fig. 6). The major compounds with highest retention time of 34.775 is 2(1H)naphthalenone, 3,5,6,7,8,8a-hexahydro-4,8a-dimethyl-6-(1-methylethenyl), followed by 34.632 for (3S,8S,9S,10R,13R,14S,17R)-17-((2R,5R). The largest peak obtained at the retention time of 33.926 for the compound olean-12-en-28-al, cyclic 1,2-ethanediyl mercaptal, the second largest peak at retention time of 22.521 for the compound carbonic acid, but-3-yn-1-yl hexadecyl ester. The other peaks were tabulated. The compound *n*-hexadeconic acid presence is responsible for antimicrobial and antioxidant activity with a retention time of 20.286. The result of the presence of compound correlates with the previous study [35].

Biosynthesis of silver nanoparticles (Ag NPs): Silver nanoparticles were synthesized using the aqueous extract of *D. quercifolia* (L.) J. Sm. tuber. The formation of Ag NPs was initially confirmed through visual observation. The plant extract appeared brown in colour and upon the addition of $AgNO_3$ solution, the reaction mixture gradually changed to a dark brown color after incubation for about 2 h, indicating the reduction of Ag^+ ions and the formation of Ag NPs.

TABLE-2
LIST OF BIOACTIVE COMPOUNDS IDENTIFIED THROUGH GC-MS ANALYSIS OF TUBER EXTRACT OF *Drynaria quercifolia*

Peak No.	Compound name	Area	Retention time
32	2(1*H*)Naphthalenone3,5,6,7,8,8a-hexahydro-4,8a-dimethyl-6-(1-methylethenyl)	133065	34.775
31	(3S,8S,9S,10R,13R,14S,17R)-17-((2R,5R)	445762	34.632
30	Olean-12-en-28-al, cyclic 1,2-ethanediyl mercaptal	3361301	33.926
20	Carbonic acid, but-3-yn-1-yl hexadecyl ester	59424	22.521
08	*n*-Propyl heptyl ether	1474112	13.332
07	Cyclohexane,1-(1,5-dimethyhexyl)-4-methyl	119629	11.793
03	2-Hydroxy-γ-butyrolacetone	499251	5.351
22	3-Benzyl-benzotriazin-4-one	525666	24.290
29	1-isopropenyl-4,5-dimethylbicyclo[4.3.0]nona	152489	33.666
15	Octane, 2,3,3-trimethyl-	94421	18.230
02	Phenol	59413	5.239
19	1-Hexadecanol	309114	22.347

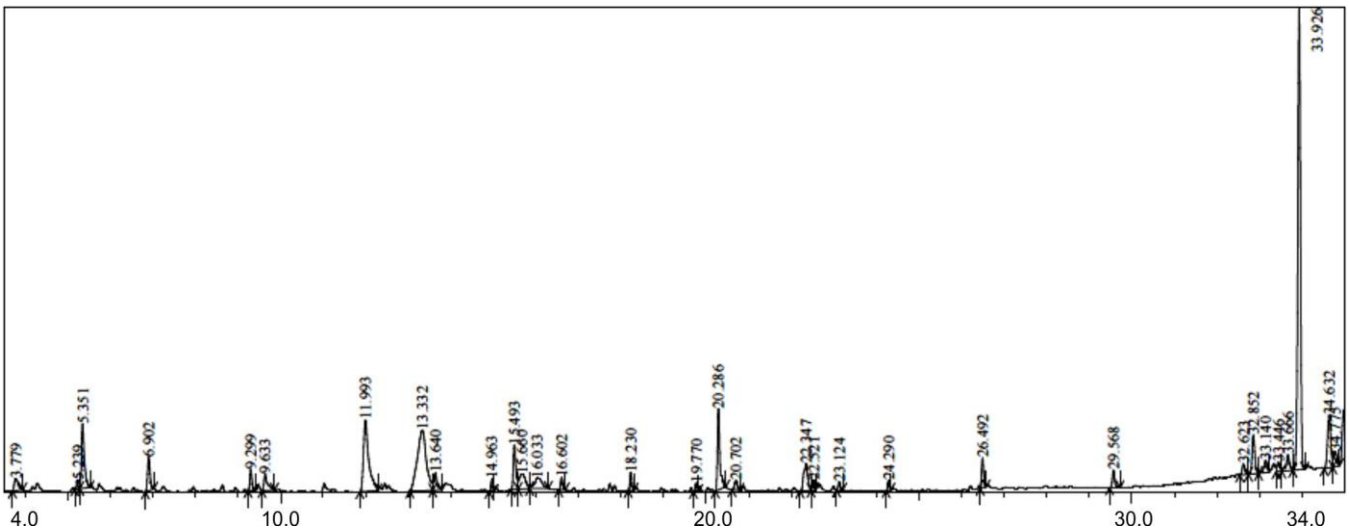

Fig. 6. GC-MS spectrum of ethanolic extract of *D. quercifolia* tuber

UV-Visible spectroscopy: The UV-Visible spectrum of the synthesized Ag NPs was recorded to monitor nanoparticle formation over time. After 72 h of reaction, a characteristic absorbance peak was observed at 445 nm (Fig. 7), which corresponds to the surface plasmon resonance (SPR) of Ag NPs and the peak appeared slightly broadened. The position and number of absorption peaks are influenced by the shape and size of the nanoparticles, particularly in the case of ellipsoidal particles. The SPR band arises due to the collective oscillation of free electrons in the metal nanoparticles when they resonate with incident light waves. The appearance and increase of this peak confirm the formation of Ag NPs in the reaction mixture. According to previous reports [36], the SPR band of Ag NPs generally occurs within the range of 435-480 nm, depending on particle concentration and size. In agreement with these findings, the present study recorded an SPR peak at 445 nm.

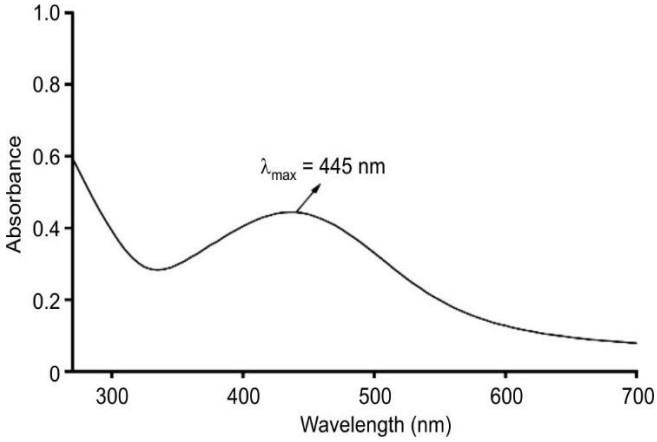

Fig. 7. UV-visible spectrum of biosynthesized Ag NPs

FTIR spectroscopy: FTIR analysis was performed to identify the functional groups involved in the reduction and stabilization of Ag NPs synthesized from the aqueous extract of *D. quercifolia*. The FTIR spectrum (Fig. 8) revealed peaks at 3733, 3572, 2629, 2566, 2260, 2164, 2061, 1973, 1542, 1025 and 742 cm^{-1}, indicating the presence of various functional groups such as carboxylic acids, amides, amines, phenols, alkanes, esters, alkyl halides and ethers. These functional groups are likely involved in the reduction of Ag^{+} ions and stabilization of the synthesized nanoparticles. Similar observations have been reported in the biosynthesis of Ag NPs using *Acalypha indica* L. extract, where the O–H stretching band shifted from 3250 cm^{-1} in the extract to 3258 cm^{-1} in AgNPs, along with shifts in C–H and C–O bands, suggesting interaction of phytochemicals with Ag NPs through reduction and adsorption processes, mainly attributed to the various alkaloid compounds [37].

X-ray diffraction analysis: The XRD pattern of the Ag NPs at 2θ in the angle range of 10º-80º using a powder X-ray diffractometer are shown in Fig. 9. A crystalline phase is suggested by a clear, sharp peak between 30º and 35º. The existence of an amorphous or mixed-phase material is indicated by the broad background signal and additional tiny peaks. An amorphous or nanocrystalline phase is suggested by the wide hump in the backdrop. The size, purity and crystalline structure of the produced Ag NPs were evaluated by

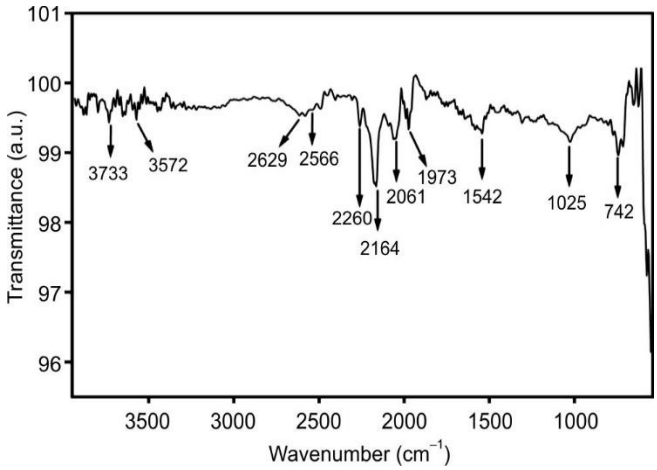

Fig. 8. FTIR analysis of biosynthesized Ag NPs

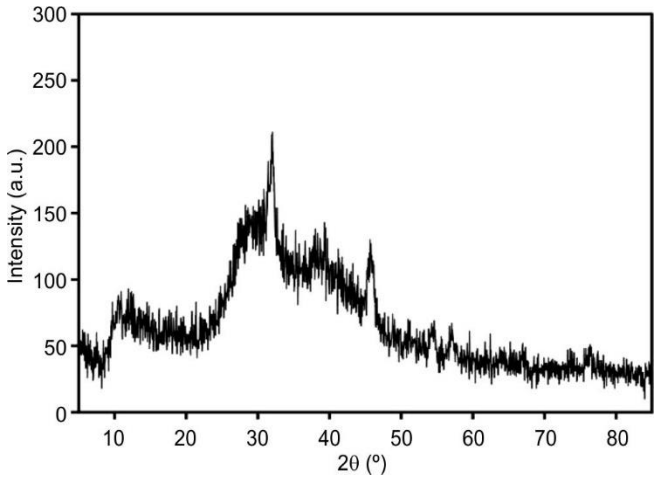

Fig. 9. XRD pattern of biosynthesized Ag NPs

XRD analysis. The powerful peak for the plane and its narrow full width at half maximum demonstrated outstanding crystalline quality, confirming the crystalline nature of Ag NPs [38].

Scanning electron microscopy (SEM): The SEM micrographs (Fig. 10) at different magnifications of 25,000× and 150,000× revealed that the synthesized Ag NPs from the tuber extract of *D. quercifolia* exhibited varied shapes, including crystalline, irregular and spherical forms, with particle sizes ranging from 20-90 nm. The clustered and rough morphology observed suggests potential applications in areas such as catalysis, sensing and surface coatings. These findings are consistent with previous reports on the green synthesis of Ag NPs using polysaccharides from *Caulerpa racemosa*, which exhibited diverse morphologies including spherical, rhomboidal and square shapes, with particle sizes ranging from 32-77 nm and an average size of about 30 nm [36].

EDX spectroscopy: The EDX spectrum (Fig. 11) shows distinct peaks corresponding to the elements present in the sample. A prominent peak observed at around 3 keV confirms the strong presence of silver (Ag), indicating the successful formation of Ag NPs. In addition to silver, smaller peaks corresponding to carbon (C), oxygen (O) and nitrogen (N) were also detected, which may originate from the biomolecules of the plant extract acting as stabilizing and capping agents during nanoparticle synthesis. Similar findings were

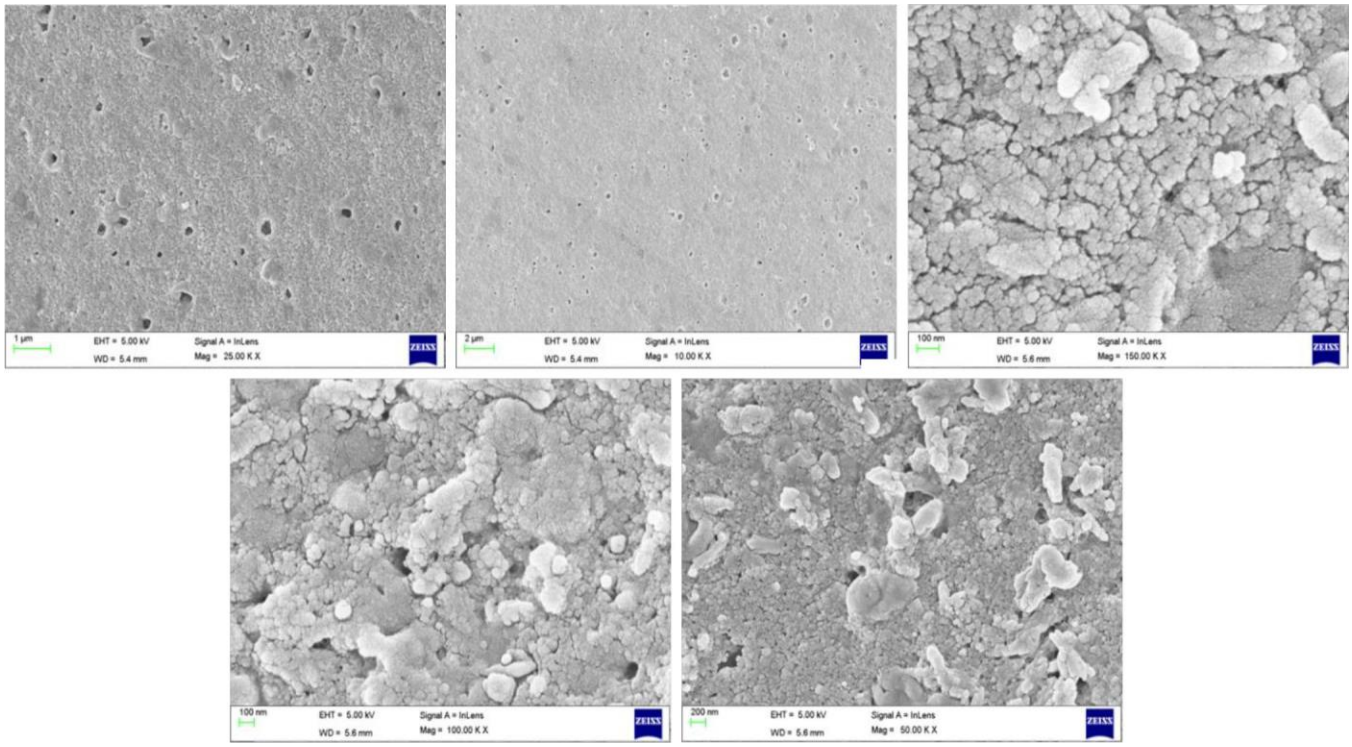

Fig. 10. SEM images of biosynthesised Ag NPs

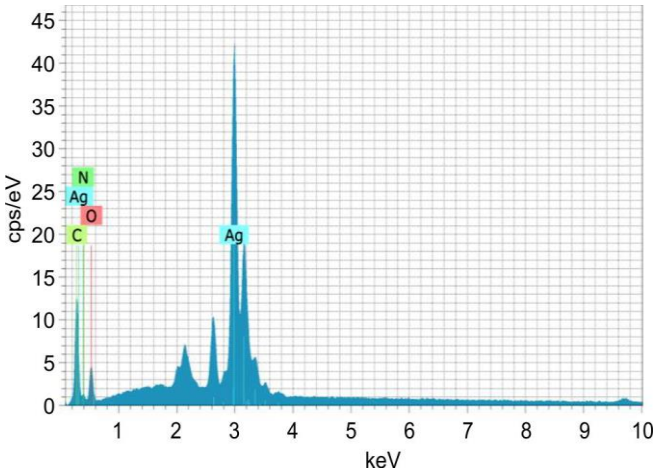

Fig. 11. EDAX spectrum of biosynthesized Ag NPs

reported by Velmani *et al.* [38], where EDX analysis of Ag NPs synthesized using *Pandanus dubius* extract revealed a major silver peak along with minor amounts of carbon, oxygen and chlorine. The relatively higher carbon and oxygen signals further suggest that organic constituents of the plant extract played an important role in the reduction and stabilization of the nanoparticles during synthesis.

***In vitro* cytotoxic studies:** The cytotoxic effect of green synthesised Ag NPs from *D. quercifolia* was assessed against HepG2 cells. After 24 h incubation with different concentration of Ag NPs potentially decreased the cell viability of HepG2 cells with the IC_{50} value of 28.18 μg/mL. The results (Figs. 12 and 13) clearly indicated that the varying concentration (6.5, 12.5, 25, 50 and 100 μg/mL) of Ag NPs treatment was significantly inhibit the proliferation of HepG2 cells in a dose dependent manner. The cellular uptake and cytotoxic effect of nanoparticles depend largely on their physicochemical properties such as size, surface charge and aggregation. Based on the SEM analysis, the size of synthesized AgNPs ranged from 20-90 nm, a size that facilitates efficient cellular entry through diffusion or membrane channels. This small particle size likely enhanced interaction with HepG2 cells, resulting in the dose-dependent reduction in cell viability observed in the cytotoxicity assay, thereby confirming the biological activity of the synthesized nanoparticles [39]. This finding is supported by a previous study in which Ag NPs synthesized using the ethanolic extract *of Chlorophytum comosum* exhibited significant cytotoxic activity against liver cancer cells, with an IC_{50} value of 98.07 μg/mL. The variation in inhibitory concentration among different studies may be attributed to differences in phytochemical constituents present in the plant sources used for the synthesis of Ag NPs [20].

The cytotoxic effect of synthesised Ag NPs against normal liver cell lines, after 24 h of incubation with different concentration of Ag NPs was also assessed for toxicity in THLE-2 cell lines. The results showed that 12.5 μg/mL of Ag NPs showed 98% of cell viability, similarly as the concentration of nanoparticles increased by 25, 50, 100 and 200 μg/mL the cell viability decreases upto 95% (Figs. 14 and 15). The combined effect of Ag NPs/CDDP was more hazardous than single exposures for both cell lines and toxicological interactions were identified in the majority of groups. Exposure to Ag NPs and a lower CDDP concentration (10 μM) was particularly noteworthy. The combination of medications reduced the viability of HepG2 cells by 50%, although normal THLE2 cells lost only about 20%. Using a higher dose of CDDP (40 μM) balanced the response to exposure between the cell lines,

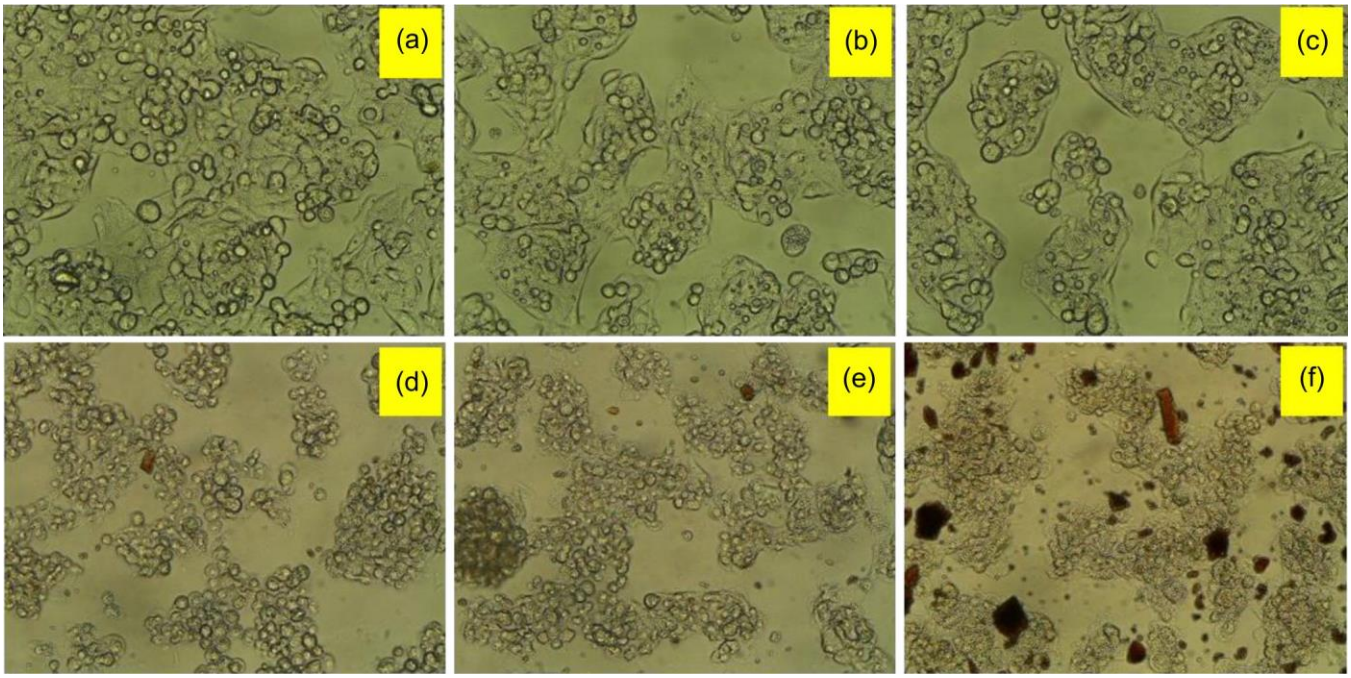

Fig. 12. Optical microscopy images showing cytotoxic effect of biosynthesized Ag NPs from *D. quercifolia* (L.) J. Sm. tuber on Hep G2 cells at different concentrations: (a) control, (b) 6.5, (c) 12.5, (d) 25, (e) 50 and (f) 100 μg/mL

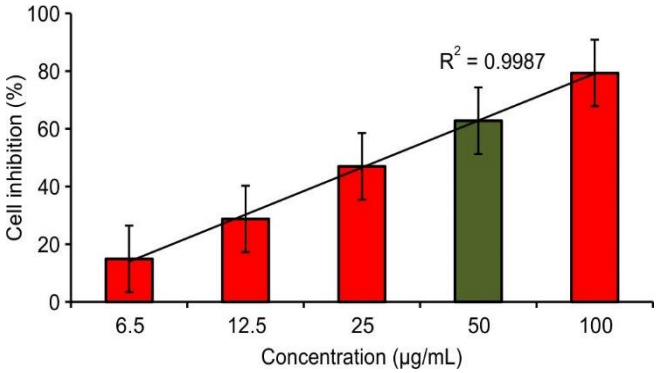

Fig. 13. Cytotoxic effect of different concentration of biosynthesised Ag NPs

exceeding the threshold for inhibiting the malignant cell line relative to the normal cell line [40].

The biochemical indicators, such as LDH activity, TAS and TOS, the cytotoxic and oxidative reactions of HepG2 and THLE2 cells to methanol and water extracts of *C. demersum* were methodically assessed. The results showed both extracts caused concentration-dependent changes in cellular viability and redox balance, with water extracts generally showing stronger effects, especially at higher dosages [41].

Apoptotic effect: Apoptotic, necrotic and normal cells were distinguished using the combination AO/ET staining technique. The dual AO/ETBR fluorescence staining method was used to identify morphological alterations in cell membranes linked to apoptosis after chemopreventive Ag NPs treatment. According to the findings, untreated control cells became green, indicating that their nuclear structure remained unchanged. However, extensive apoptosis was apparent after Ag NPs treatment, as shown by reddish-orange fluorescence (Fig. 16). The present findings are correlated with Palanisamy *et al.* [42] stated that aqueous extract of *Momordica charantia* L. based synthesised Ag NPs attained potent cytotoxic activity against breast cancer cell lines (MCF7) through apoptosis, which was confirmed by AO/ET dual staining. Cell shrinkage, chromatin condensation and inter-nucleosomal fragmentation were among the alterations in AgNP-treated cells that demonstrated the treatment's effect on cell morphology. This analysis indicates the tested extract's possible impact on cell structure and shows its significance in relation to apoptosis.

Mitochondrial membrane potential (MMP) assay: Nanosilver is known to damage cellular membranes, increase membrane permeability and induce intracellular calcium overload, which leads to excessive generation of reactive oxygen species (ROS) and alterations in mitochondrial membrane potential [43]. In apoptotic cells, the collapse of mitochondrial membrane potential causes the JC-10 dye to lose its aggregated form and revert to its monomeric green form in the cytoplasm. In the present study, HepG2 cells treated with Ag NPs showed both green and red fluorescence, indicating loss of mitochondrial membrane potential, whereas control cells mainly exhibited normal fluorescence (Fig. 17). This suggests that Ag NPs treatment disrupts mitochondrial function and triggers apoptosis. Similar findings have been reported for green synthesised Ag NPs from the marine mangrove plant *Avicennia marina*, which demonstrated strong cytotoxic activity against A549 cells through mitochondrial-mediated cell death, confirmed using rhodamine 123 staining of damaged mitochondrial membranes in cancer cells [44].

Conclusion

The present investigation suggests that the tuber extract of *D. quercifolia* acts as an effective reducing and stabilizing agent for the synthesis of silver nanoparticles (Ag NPs). Various techniques including UV-Visible spectroscopy, XRD, SEM and EDX, confirmed the successful formation and trans-

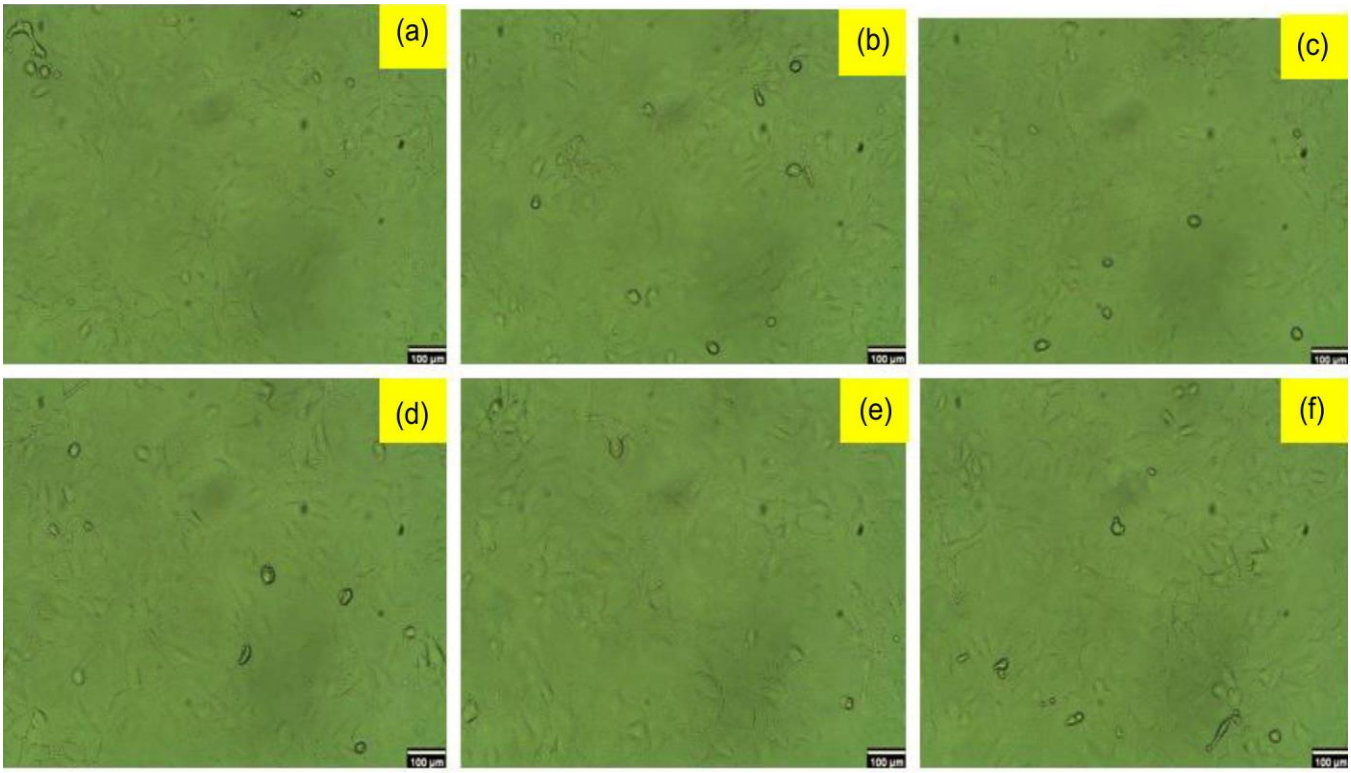

Fig. 14. Optical microscopy images showing cytotoxic effect of biosynthesized AgNPs from *D. quercifolia* (L.) J. Sm. tuber on THLE-2 normal cells at (a) 12.5, (b) 25, (c) 50, (d) 100, (e) 200 µg/mL and (f) control

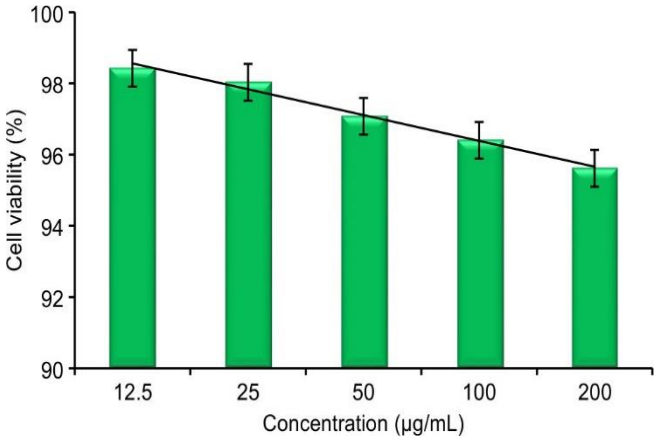

Fig. 15. Cytotoxic effect of different concentration of synthesised Ag NPs synthesised from aqueous extract of *D. quercifolia* (L.) J.Sm. tuber. in THLE-2 cell lines

formation of the nanomaterial, while the presence of different functional groups in the plant extract facilitated the reduction of Ag^{+} ions into Ag^{0}. Furthermore, the synthesized Ag NPs exhibited significant cytotoxic activity against HepG2 cells through a mitochondrial-mediated apoptotic pathway. These findings indicate that Ag NPs synthesised from *D. quercifolia* tuber extract possess promising anticancer potential against HepG2 liver cancer cells.

CONFLICT OF INTEREST

The authors declare that there is no conflict of interests regarding the publication of this article.

DECLARATION OF AI-ASSISTED TECHNOLOGIES

During the preparation of this manuscript, the authors used an AI-assisted tool(s) to improve the language. The authors reviewed and edited the content and take full responsibility for the published work.

REFERENCES

1. M. Fahim, A. Shahzaib, N. Nishat, A. Jahan, T.A. Bhat and A. Inam, *JCIS Open*, **16**, 100125 (2024); https://doi.org/10.1016/j.jciso.2024.100125
2. A. Saravanan, P.S. Kumar, S. Karishma, D.V.N. Vo, S. Jeevanantham, P.R. Yaashikaa and C.S. George, *Chemosphere*, **264**, 128580 (2021); https://doi.org/10.1016/j.chemosphere.2020.128580
3. P. Makvandi, C.Y. Wang, E.N. Zare, A. Borzacchiello, L.N. Niu and F.R. Tay, *Adv. Funct. Mater.*, **30**, 1910021 (2020); https://doi.org/10.1002/adfm.201910021
4. J.J. Xu, W.C. Zhang, Y.W. Guo, X.Y. Chen and Y.N. Zhang, *Drug Deliv.*, **29**, 664 (2022); https://doi.org/10.1080/10717544.2022.2039804
5. M. Rafique, I. Sadaf, M.S. Rafique and M.B. Tahir, *Artif. Cells Nanomed. Biotechnol.*, **45**, 1272 (2017); https://doi.org/10.1080/21691401.2016.1241792
6. R.K. Das, V.L. Pachapur, L. Lonappan, M. Naghdi, R. Pulicharla, S. Maiti, M. Cledon, L.M.A. Dalila, S.J. Sarma and S.K. Brar, *Nanotechnol. Environ. Eng.*, **2**, 18 (2017); https://doi.org/10.1007/s41204-017-0029-4
7. R. Kumar, M. Kumar, S. Kumar and A. Kumar, *Case Studies Chem. Environ. Eng.*, **4**, 100195 (2021); https://doi.org/10.1016/j.crgsc.2021.100195
8. V. Sharma, P. Kaushik, D. Kumar and S. Sharma, *ACS Omega*, **5**, 10919 (2020); https://doi.org/10.1021/acsomega.0c01136

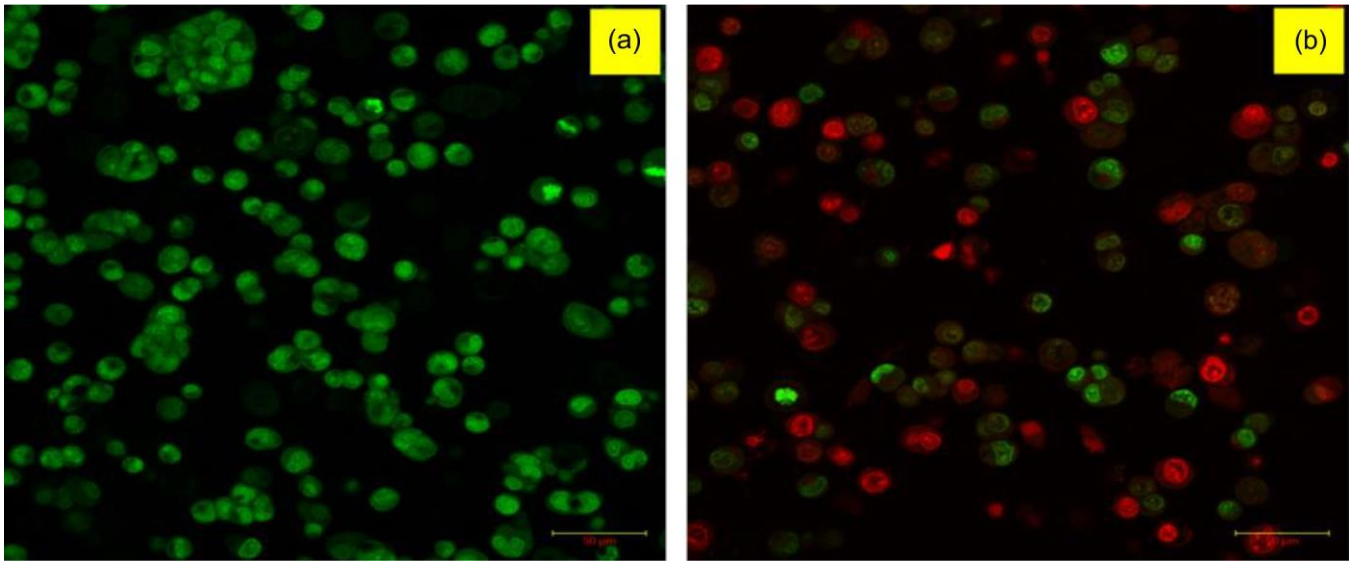

Fig. 16. Effects of AgNPs synthesised AgNPs synthesised from aqueous extract of *Drynaria quercifolia* (L.) J.Sm. tuber treatment after 24 h on apoptosis effect on HepG2 cells assessed by AO/EB staining; (a) control and (b) 123.29 µg/mL AgNP exposure.

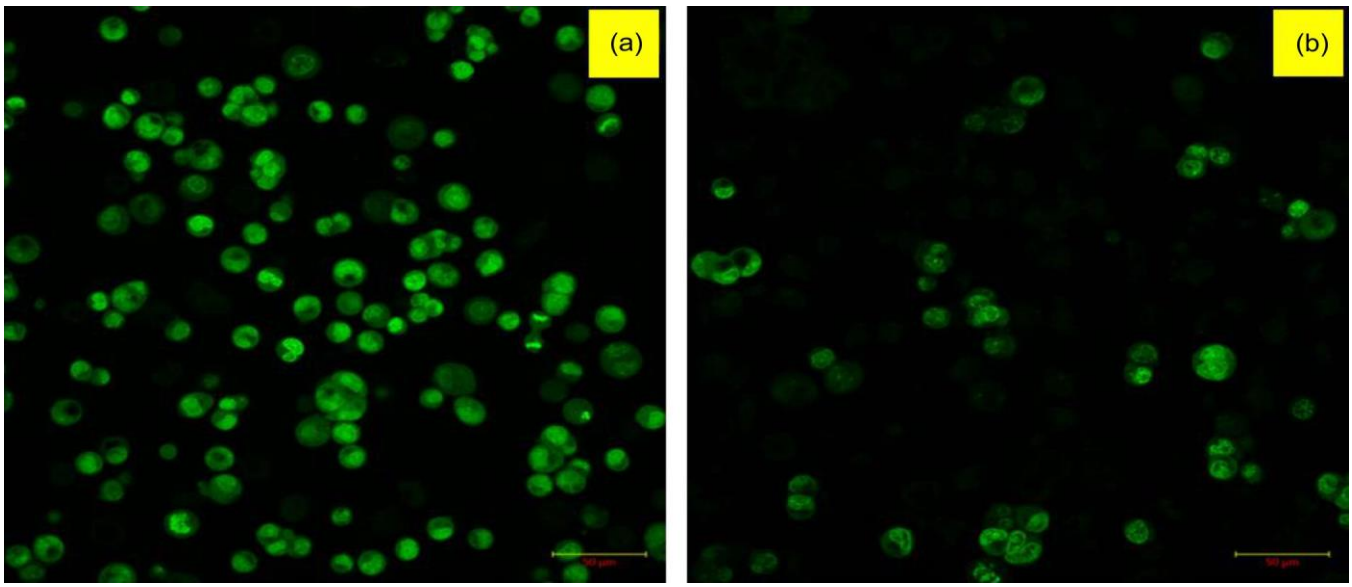

Fig. 17. Effects of synthesised AgNPs synthesised from aqueous extract of *Drynaria quercifolia* (L.) J.Sm. tuber treatment after 24 h on mitochondrial membrane potential of HepG2 cells assessed by JC-10 dye staining; (a) control and (b) 123.29 µg/mL AgNP exposure

9. S. Shahzadi, S. Zafar, M. Iqbal, M.A. Iqbal and A. Shah, *RSC Adv.*, **15**, 3858 (2025); https://doi.org/10.1039/D4RA07519F
10. Vidyasagar, R.R. Patel, S.K. Singh and M. Singh, *Mater. Adv.*, **4**, 1831 (2023); https://doi.org/10.1039/D2MA01105K
11. M. Dyusebaeva, D. Berillo, Z. Yesbussinova, N. Ibragimova, D. Shepilov, S. Sydykbayeva, A. Almabekova, N. Chinibayeva, A.O. Adeloye and G. Berganayeva, *Int. J. Mol. Sci.*, **26**, 7499 (2025); https://doi.org/10.3390/ijms26157499
12. L.H. Swift and R.M. Golsteyn, *Int. J. Mol. Sci.*, **15**, 3403 (2014); https://doi.org/10.3390/ijms15033403
13. F. Bray, J. Ferlay, I. Soerjomataram, R.L. Siegel, L.A. Torre and A. Jemal, *CA Cancer J. Clin.*, **68**, 394 (2018); https://doi.org/10.3322/caac.21492
14. A. Vickers, *CA Cancer J. Clin.*, **54**, 110 (2004); https://doi.org/10.3322/canjclin.54.2.110
15. B. Wang, S. Hu, Y. Teng, J. Chen, H. Wang, Y. Xu, K. Wang, J. Xu, Y. Cheng and X. Gao, *Signal Transduct. Target Ther.*, **9**, 200 (2024); https://doi.org/10.1038/s41392-024-01889-y
16. M.J. Nirmala, U. Kizhuveetil, A. Johnson, G. Balaji, R. Nagarajan and V. Muthuvijayan, *RSC Adv.*, **13**, 8606 (2023); https://doi.org/10.1039/D2RA07863E
17. D. Hazarika, S. Sarma and P. Shankarishan, *BioTechnologia*, **105**, 287 (2024); https://doi.org/10.5114/bta.2024.141807
18. S. Raj, R. Trivedi and V. Soni, *Surfaces*, **5**, 67 (2021); https://doi.org/10.3390/surfaces5010003
19. M. Wang and M. Thanou, *Pharmacol. Res.*, **62**, 90 (2010); https://doi.org/10.1016/j.phrs.2010.03.005
20. P. Singh, Y.J. Kim, D. Zhang, and D.C. Yang, *Trends Biotechnol.*, **34**, 588 (2016); https://doi.org/10.1016/j.tibtech.2016.02.006
21. N. Aziz, M. Faraz, M.A. Sherwani, T. Fatma and R. Prasad, *Front. Chem.*, **7**, 65 (2019); https://doi.org/10.3389/fchem.2019.00065
22. N. Ramesh, M.B. Viswanathan, A. Saraswathy, K. Balakrishna, P. Brindha and P. Lakshmanaperumalsamy, *Fitoterapia*, **72**, 934 (2001); https://doi.org/10.1016/S0367-326X(01)00342-2

23. A.A. Devanesan, D. Garlapati, S.V.P.I. Abraham, S. Gnanaselvan, A.S. Ameer, A. Chandran, R. Veerapandian, S. Sundan, S. Nandakumar, R. Rajamanickam and M. Vijayaraghavan, *Plant Biosystems*, **159**, 668 (2025); https://doi.org/10.1080/11263504.2025.2496477
24. J.F. Runa, M. Hossain, M. Hasanuzzaman and M.R. Ali, *Adv. Pharm. Bull.*, **3**, 465 (2013).
25. D. Peach and M.V. Tracey, Modern Methods of Plant Analysis, Springer Berlin, Verlag., edn 4, pp. 373-374 (1995).
26. N. Raman, Phytochemicals techniques, New India Publishing Agency, New Delhi, pp. 19-25 (2006).
27. M.S. Gião, M.L. González-Sanjosé, M.D. Rivero-Pérez, C.I. Pereira, M.E. Pintado and F.X. Malcata, *J. Sci. Food Agric.*, **87**, 2638 (2007); https://doi.org/10.1002/jsfa.3023
28. F. Liu, V.E.C. Ooi and S.T. Chang, *Life Sci.*, **60**, 763 (1997); https://doi.org/10.1016/S0024-3205(97)00004-0
29. M.P. Madan, G. Raghavan, K.S.R. Ajay and P. Prabhu, *Acta Pharm.*, **55**, 297 (2005).
30. N. Horiuchi, K. Nakagawa, Y. Sasaki, K. Minato, Y. Fujiwara, K. Nezu, Y. Ohe and N. Saijo, *Cancer Chemother. Pharmacol.*, **22**, 246 (1988); https://doi.org/10.1007/BF00273419
31. C. Sivaraj, Y. Aashinya, R. Sripriya and P. Arumugam, *Free Radic. Antioxid.*, **8**, 26 (2018)
32. A.M. Najafabad and R. Jamei, *Avicenna J. Phytomed.*, **4**, 343 (2014).
33. S.B. Rao, M. Jayanthi, R. Yogeetha, H. Ramakrishnaiah and J. Nataraj, *J. Appl. Pharm. Sci.*, **3**, 203 (2013).
34. K.I. Berker, K. Güçlü, İ. Tor and R. Apak, *Talanta*, **72**, 1157 (2007); https://doi.org/10.1016/j.talanta.2007.01.019
35. G. Prasanna and M. Chitra, *Am. J. Adv. Drug Deliv.*, **3**, 72 (2014).
36. C. Ragunath, K. Madeshwaran, D. Paulraj, S. Murugesan and R. Venkatachalam, *Next Nanotechnology*, **6**, 100088 (2024); https://doi.org/10.1016/j.nxnano.2024.100088
37. L. Madaniyah, S. Fiddaroini, E.K. Hayati, M.F. Rahman and A. Sabarudin, *OpenNano*, **21**, 100220 (2025); https://doi.org/10.1016/j.onano.2024.100220
38. S. Velmani, E.N. Sholkamy, P. Ruba, S. Kanaga, V. Balamurugan, M.A. Tarighat and G. Abdi, *Sci. Rep.*, **15**, 39940 (2025); https://doi.org/10.1038/s41598-025-23717-1
39. A.K. Suresh, D.A. Pelletier, W. Wang, J.L. Morrell-Falvey, B. Gu and M.J. Doktycz, *Langmuir*, **28**, 2727 (2012); https://doi.org/10.1021/la2042058
40. R. Rank Miranda, M. Pereira da Fonseca, B. Korzeniowska, L. Skytte, K.L. Rasmussen and F. Kjeldsen, *J. Nanobiotechnol.*, **18**, 164 (2020); https://doi.org/10.1186/s12951-020-00719-x
41. M. Ari, B. Emsen, M. Dogan and K. Sarlar, *Research Square (preprint)* (2025); https://doi.org/10.21203/rs.3.rs-7511345/v1
42. S. Palanisamy, R. David, E. Madav, V. Devi Kannan, V. Rajendran, S. Sampath, M. Z. Ahmed, A. S. Alqahtani, S. Kazmi and P. Asaithambi, *Mater. Technol.*, **39**, 2304428 (2024); https://doi.org/10.1080/10667857.2024.2304428
43. D. McShan, P.C. Ray and H. Yu, *J. Food Drug Anal.*, **22**, 116 (2014); https://doi.org/10.1016/j.jfda.2014.01.010
44. S. Tian, K. Saravanan, R.A. Mothana, G. Ramachandran, G. Rajivgandhi and N. Manoharan, *Saudi J. Biol. Sci.*, **27**, 3018 (2020); https://doi.org/10.1016/j.sjbs.2020.08.029